Magnetoinductive Waves and Wireless Power Transfer

Christopher J. Stevens

***Abstract*—Recent research in wireless power transfer has highlighted the potential benefits for relaying power from source to receiver by a number of resonating relay coils coupled via mutual inductance. A number of researchers have reported experimental systems based on relay coils and have noted that power transfer efficiency to loads located at different points on the structure can vary widely. Such structures, often known as magnetoinductive waveguides are well known to carry signals known as magnetoinductive waves (MIW) when excited with a frequency in their passband. This paper presents an investigation into their impact on wireless power systems and methods by which negative effects may be minimized. Using the physics of magnetoinductive waves it becomes possible to understand the behavior of relay coil systems and to model them in a closed form. The effects of reflections and standing waves on a one-dimensional system are considered and their effect on the input impedance and the variation of matching conditions determined. An optimum receiver load is proposed based on the results and tested experimentally. A simple experimental demonstrator is used as a model for study, which achieves 58% efficient power transfer to a single load at any point on its length.**

***Index Terms*—Magnetic metamaterial, near field coupling, relay coil, wireless power transfer.**

I. Introduction

WIRELESS power transfer is an old topic [1] of much current interest [2], [3] with significant competition between standards and approaches. Most approaches utilize electromagnetic induction to carry power from a transmitting coil to one or more receiving units. Operation frequencies between 100 kHz and tens of megahertz have been considered [3], [4] with the license free ISM bands at 6.78 and 13.56 MHz being attractive choices, metamaterials have been demonstrated to usefully contribute to these systems by helping to concentrate magnetic flux on its way from transmitter to receiver [5] but have not themselves been widely considered as power delivery channels [6], [7].

Following the original work on two terminal systems [2], where a power source drives a resonant transmitting antenna delivering power to a load via a single receiving coil, a number of researchers have considered approaches for increasing the range of efficient power transfer [8]. Several methods have been employed to increase the range including impedance matching [9] and notably the use of passive, resonant, relay coils to increase the oscillating magnetic flux at the receiving antenna. There are two main configurations for these relays that have been studied axial [10] and planar [11], [12]. In general, the relays considered in all these works are of similar size to the source and receive coils and transfer power by mutual magnetic coupling [13] their mutual inductance. In most cases, the size of the coils is much smaller than the vacuum wavelength at the power transfer frequency and, hence, it is generally assumed that radiation by any of the individual coils is negligible.

These conditions, electrically small resonators, coupled together in a regular periodic fashion, are essentially the same as those describing another recent innovation magnetic metamaterial structures known as magnetoinductive waveguides [14]. In general, metamaterials are repeating arrays of resonant electromagnetic elements and in this paper, we are concerned with magnetically active varieties [15]. Periodic arrays of coupled circuits, such as those employed in metamaterials generally support several modes of signal propagation. In 2002, magnetic metamaterials were discovered to exhibit a novel type of wave propagation known as a magnetoinductive wave (MIW) [14] which may only propagate within its host metamaterial.

In the past work, metamaterials have been considered as novel waveguides [16] carrying MIWs, for distributed broadband data transfer systems [15], [17] and to carry signals in MRI imaging [18]. A significant advantage of this type of waves for power transfer is their strongly magnetic character, which leads to efficient coupling to resonant electric circuits in their near field. By their very nature, MIW with strong coupling offers low loss and wide bandwidth channels [19]. Thus, a good power transfer structure would be generally well prepared to offer a high-bandwidth communication channel with data capacity well above traditional near field coupling systems.

Most researchers have considered 1-D arrays of relay coils excited at one end by a source antenna driving a single load located at the other. In such configurations, with perfectly matched terminals, waves are launched by the source, traverse the structure, experiencing loss due to the resistance of each relay coil, and are absorbed by the receiver as considered in [11] among others.

In this paper, we consider something more reminiscent of a tapped transmission line, where receiving terminals may be coupled to any of the resonators in a line such as the general system shown in Fig. 1(c). Here, the source drives one end of a line, but in general it could be located at any cell (in this paper, each relay coil or resonator is referred to as a cell of the magnetoinductive waveguide known as the line). In such systems,

Manuscript received September 30, 2014; accepted November 4, 2014. Date of publication November 11, 2014; date of current version July 10, 2015. This work was supported by the Oxford University and ISIS Innovations for this research. Recommended for publication by Associate Editor J. T. Boys.

The author is with the Department of Engineering Science, Oxford University, Oxford OX1 3PJ, U.K. (e-mail: chris.stevens@eng.ox.ac.uk).

Color versions of one or more of the figures in this paper are available online at http://ieeexplore.ieee.org.

Digital Object Identifier 10.1109/TPEL.2014.2369811

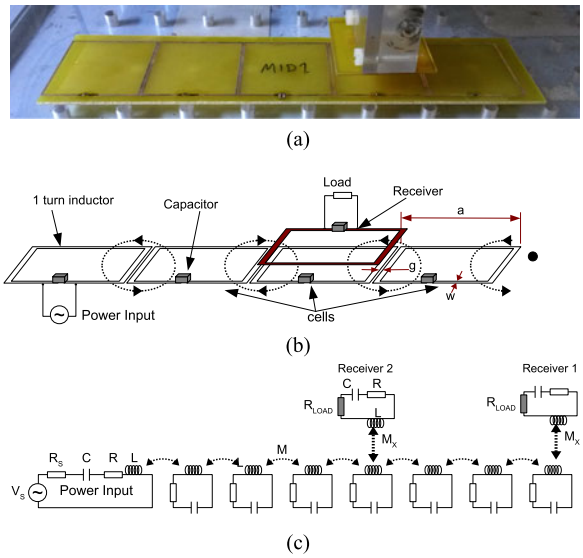

Fig. 1. (a) Photograph of a simple planar 1-D magnetoinductive waveguide and a receiver placed above it. (b) Diagram showing the configuration of the inductors, their mutual inductive coupling, and capacitors to tune the structure. (c) Circuit diagram of a similar line with a source driving the first cell and two receivers taking power, one at the line end and the other at another cell between source and termination.

standing MIWs may become a problem, as waves arriving at the last cell in a line from a source are reflected back toward the source.

A number of studies have noted the presence of these standing wave effects, for instance, Zhong *et al.* [10] use a load driven at a number of different locations around a ring of relay coils and find that loading certain relay coils results in very poor performance, while in others high efficiency is possible. Most modeling in this area uses circuit techniques and often relies on the numerical inversion of impedance matrices (which are often quite large for long sequences of relays). In this paper, a new method is explored, using the properties of MIWs to enable the derivation of a relatively simple set of equations. These can model relay sets of any length without need for matrix or numerical approaches to provide insight into the optimization of relay coil systems.

In Section II, the method exploiting the properties of MIW is derived. First, the reflectance for MIW from a termination is derived and from this, using the propagation of MIW the standing wave amplitude can be obtained. To avoid the use of a continuous fraction, a method is invented to determine the effective impedance of an arbitrary line length using the MIW reflectances. Incidental to this, a general solution to the continuous fraction is obtained. From this composite reflectance, the optimal load impedance can be derived for any receiver. Finally, the net input impedance of the line with load is determined and power transfer efficiency derived.

Section III reports to results of a simple experimental MIW power transfer system and compares them to the predictions of the analytical model and considers the potential improvement that would arise from providing modulation of the line termination condition.

Section IV reports the key conclusions and outcomes of the work along with recommendations for a simple design strategy for implementation of MIW power transfer lines.

II. MIWs, Defects, and Power Transfer

Metamaterials for RF frequencies are generally formed using periodic arrays of resonant circuits (cells). Magnetic metamaterials (being those designed to exhibit a strong magnetic permeability) utilize simple series resonant circuits (Inductance *L*, Resistance *R*, and Capacitance *C*), which are often coupled together via the mutual inductance between adjacent cells. Fig. 1(a) shows a typical 1-D metamaterial structure, whose cells are square pcb tracks with series capacitors bridging a small gap in the conductors forming the *LC* resonator tuned to a common resonant frequency.

The cells are very close to one another so that a current circulating in one cell generates a significant magnetic flux through the neighboring cells and, hence, they are coupled via a mutual inductance *M*. If a resonant current is induced in one cell and the mutual inductance results in a current being stimulated in the cells neighbors. These in turn stimulate their neighbors and this is the propagation of a MIW [14]. A key feature of these structures is that they are open: the magnetic flux linking the cells extends beyond the structure and provides a region of near field from which nearby structures can draw power or data signals.

The power transfer devices which are the subject of this paper are formed by connecting an RF source directly to one of the cells of a conventional planar MIW guide as shown in Fig. 1(b). Power is then delivered to one or more receivers in the near field of the guide.

A. MIWs

Detailed descriptions of the properties of MIWs can be found in the literature [14], [19]–[21] and need not be repeated here. We include the key results below. In general, there is a limited bandwidth available for signal transmission via this type of channel with the bandwidth increasing as the cells' mutual inductance coupling rises, while the losses commensurately decrease. In consequence, the optimal structure for both power and high bit rate data transfer requires that the mutual inductive coupling between cells be as high as possible. This coupling is usually characterized by the parameter $k = 2M/L$, where M is the nearest neighbor mutual inductance and L is the self-inductance of each cell. In the planar cases, k is generally negative although designs have been presented with near planar character and positive k [22].

MIW are described in terms of the currents circulating in each cell (I_n for the nth cell) and the general expression for a MIW in 1-D is $I_n = I_0^{-\gamma nd} = I_0 e^{-\alpha nd - j\beta nd}$, where γ is the propagation constant, α is the attenuation, and β is the phase factor. Attenuation at the cells resonant frequency is then given by (1), where αd is the attenuation per cell for MIW transmission (in a structure with a period of d and Q is the individual cell's resonant quality factor measured in isolation [19]). Here, η is the number of spatial dimensions occupied by the lattice. For a

line of cells, this is 1 and for 2-D planar array of cells it is 2

$$\alpha d = \sin h^{-1}\left(\frac{1}{\eta k Q}\right). \tag{1}$$

Its clear from (1) that for efficient power transmission in this medium, strong coupling (high k) and low loss (high Q) resonators are preferred. Hence, in optimizing metamaterial power transfer designs, care should be taken that the figure of merit be as high as possible. Designs should thus maximize mutual inductance between cells while minimizing the series resistance of each cell. The form of kQ shows that low-frequency systems operating in the submegahertz regime would require a much larger mutual inductive coupling for high efficiency than those designed at higher frequencies. Most demonstrations for low-frequency relay systems [10], [23] use wound high-inductance coils with large self-inductance often as much greater than 1 μH.

Propagation for waves in such a very low loss, 1-D system is governed by a simple dispersion equation

$$\cos(\beta d) = \left(\frac{\omega_0^2 - \omega^2}{k\omega^2}\right) \tag{2}$$

where ω_0 is the cell resonant angular frequency $\omega_0 = 1/\sqrt{LC}$. The band limits for MIW transmission are then defined by the frequencies for which $|\cos(\beta d)| = 1$. This provides a simple expression for the bandwidth which is shown in

$$\frac{\Delta\omega}{\omega_0} = \frac{1}{\sqrt{1-\eta k}} - \frac{1}{\sqrt{1+\eta k}}. \tag{3}$$

For example, in a 1-D structure ($\eta = 1$) with $|k| = 0.1$, the bandwidth available for MIW transmission will be 10% of the cell resonance, while if the coupling rises to $|k| = 0.6$ the fractional bandwidth increases to 79%. At $k = 1$, the upper bound of bandwidth becomes infinite, which is theoretically possible but has so far proved hard to achieve [24].

B. Calculating Input Impedance via MIW Reflectance

The key thrust of this paper is to obtain an analytical expression or equation set that can predict the efficiency for any 1-D planar or axial relay coil system, for power transfer to a receiver located on any cell. To this end, we need to find power injected and power delivered, accounting for the impact of standing MIW and any terminating loads along with the individual cell parameters and their coupling.

In order to determine the power injected and delivered for an arbitrary MIW structure, one needs must consider the impedance presented to a source, the reflection of power at both the end of the line (termination), and current circulating at a cell somewhere along the line, where a load is being applied by a receiver (defect).

For a 1-D magnetoinductive waveguide, there is a simple matching condition [25] when only first order coupling is significant, which states that a structure is perfectly terminated if the last cell in a line includes an extra series impedance Z_0 given by

$$Z_0 = j\omega M e^{-(\alpha+j\beta)d} \tag{4}$$

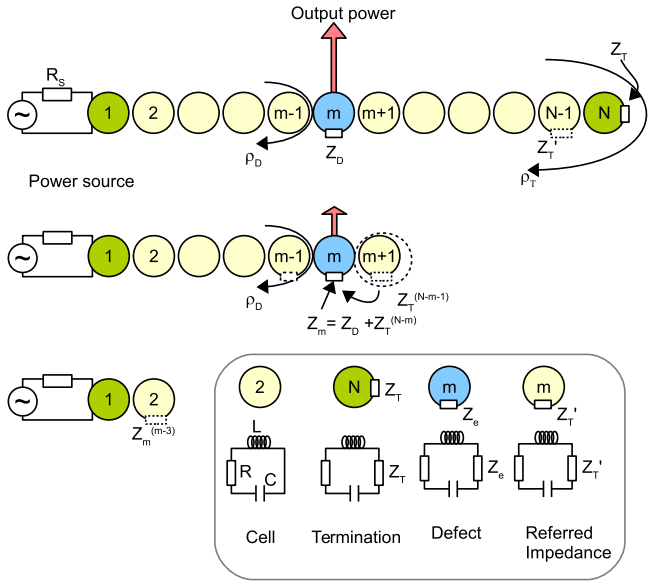

Fig. 2. Line formed from N cells, with a defect in the mth cell. The source injects power which travels along the line, partially reflects at the defect, and then continues to the end of the line, where it is reflected or absorbed as a function of the termination condition. Power is absorbed in the defect and this represents the wireless power transfer to a coupled terminal as in Fig. 1.

where $\alpha + j\beta$ are the real and imaginary components of the wave propagation function γ and d is the period of the cells. In practice broadband, matching is rather difficult to achieve as the value of Z_0 is a complex frequency-dependent function and only has a pure real value (i.e., resistive character) at ω_0, where its value is $Z_0(\omega_0) = \omega_0 M e^{\alpha d}$. For most power transfer applications, however a single frequency is quite adequate making this matching impedance the optimal load that can be used to terminate a 1-D MIW and receive maximum power at its end.

Matching a loaded receiver tapping into the MIW power at an arbitrary cell between source and termination is somewhat harder. If one considers Receiver 2 in Fig. 1(c), it can tap part of the power arriving the mth cell from the source, but that portion that continues along the line will reflect and then interfere with the incoming wave when it returns to the receiver. How much power is reflected, is transmitted or absorbed depends both on the behavior of the mth cell and on the rest of the line beyond it.

In order to obtain an analytical solution for the power transmitted to a load and the overall efficiency, one must determine the effective impedance that a line with termination presents to its source (the input impedance). This allows calculation of the power drawn from that source. One must then determine the resulting current MIW circulating in the loaded cell and hence the output power.

First, one must consider the input impedance. As shown in Fig. 2 , if the last cell in a line (cell N) includes an extra series impedance Z_T, then this will impact the nearest neighbor as though it had a load itself. The circulating currents in the last pair cells of the line are related in the first-order coupling

approximation [16] by

$$(Z + Z_T)i_N + Xi_{N-1} = 0 \tag{5}$$

$$Zi_{N-1} + X(i_N + i_{N-2}) = 0 \tag{6}$$

where X is the coupling between cells given by $X = j\omega M$ is the series impedance of a typical resonant cell $Z = R + j\omega L + 1/j\omega C$ and i_N ,i_{N-1} and $_{iN-2}$ are the currents circulating in the last three cells of the line. Combining the equations one finds

$$\left(Z - \frac{X^2}{Z + Z_T}\right) i_{N-1} + Xi_{N-2} = 0 \tag{7}$$

in which the term $-X^2/(Z + Z_T) = \omega^2 M^2/(Z + Z_T)$ is the extra impedance presented by cell N to cell $N-1$. If we were to remove the termination cell and add this impedance to next cell $(N - 1)$ the rest of the lines behavior will be unchanged. Repeating this process to consider the impact on the $N - 2$ cell and so on allows the input impedance of any length of MIW line to be calculated as a continuous fraction with the input impedance of a line p cells in length being

$$Z_T^{(p)} = \cfrac{\omega^2 M^2}{Z + \cfrac{\omega^2 M^2}{Z + \cfrac{\cdots}{\cdots + \cfrac{\omega^2 M^2}{Z + Z_T}}}}. \tag{8}$$

Until now, this expression had no simple closed form simplification, making it seem that a neat analytical optimization is impossible, however, if one considers the MIW reflection as a second method to determine the effect of the terminating load elsewhere on the line it becomes possible to obtain a solution to this problem. Most often those considering finite arrays of relay coils for wireless power and contactless data use circuit models and impedance matrix inversion [15] to obtain numerical solutions for the circulating currents in each cell and, hence, derive efficiency S_{21}, etc. Matrix methods have been shown to work very well, but do not offer the immediate insight that an analytical approach can and may not be readily generalized.

One uses the fact that the ratio between the forward and reflected MIW at any location before the termination can be related to the MIW reflectance at it. At the termination, MIW arriving with current amplitude I are reflected with amplitude R and a reflectance of $\rho_T = R/I$. The ratio between forward traveling and reflected waves at other points on the line would then be given by

$$\rho_p = \frac{Re^{-(p-1)\gamma d}}{Ie^{(p-1)\gamma d}} = \rho_T e^{-2(p-1)\gamma d} \tag{9}$$

where p is the number of cells before the termination, where we are trying to solve reflectivity. This reflectance should be identical to that produced by replacing the p cells after this point with the termination impedance referred p times according to (8). Hence, if we equate the two reflectances one can find a solution to the continuous fraction

$$\rho_{N-m} = \rho(Z_T^{(p)}) \tag{10}$$

where ρ_{N-m} is the reflectance measured at the mth cell in an N line arising from the N_{th} and $Z_T^{(p)}$ is the input impedance of that section of line between m and N produced by the terminating impedance at N. Its now only left to find the termination reflectance and determine the input impedance. To find MIW reflectance at N one can return to (5) and (6) and write each of the currents as a sum of forward and reflected waves

$$i_{N-1} = I + R = I(1 + \rho_T) \tag{11}$$

$$i_{N-2} = Ie^{\gamma d} + Re^{-\gamma d} = I(e^{\gamma d} + \rho_T e^{-\gamma d}) \tag{12}$$

where I is the forward wave amplitude arriving at the last cell before the termination, and R is the MIW amplitude reflected from it. Substituting for these expressions into (6), one obtains an expression for ρ_T as

$$\rho_T(Z_T) = \frac{X^2 - (Z + Xe^{\gamma d})(Z + Z_T)}{(Z + Xe^{-\gamma d})(Z + Z_T) - X^2}. \tag{13}$$

This is the key to obtaining a solution for $Z_T(p)$. Equation (13) can be rearranged to allow one to find the effective terminating impedance in terms of the reflectance at the mth cell which gives

$$Z_T^{(p)}(\rho_p) = \frac{X^2(1 + \rho_p)}{Z(1 + \rho_p) + X(\rho_p e^{-\gamma d} + e^{\gamma d})} - Z \tag{14}$$

where $p = N - m$. Equation (14) is then a solution to the generalized input impedance $Z_T^{(p)}$ for a finite length of MIW whose last cell is terminated with a series impedance Z_T.

A shown in Fig. 2, having referred the load to the defect cell, which is the mth cell in the line, one can now add its load Z_D in series with the referred termination impedance $Z_T^{(p)}$. The MIW has now been converted to a line of length m cells with a load $Z_M = Z_D + Z_T^{(p)}$ (second MIW line in Fig. 2).

We calculate the net reflectance from the defect (wave amplitudes at cell $m - 1$), which will be given by using $Z_T^{(p)}$ in (13). Fig. 3 shows the magnitude of the reflectance as a function of frequency across the MIW passband defined by (3) for a case, where Z_D is pure real as a function of its resistance value scaled by $\omega_0 M$. Here, the values are computed for a low loss case, where the cells have negligible resistance ($R = 10^{-1}\Omega$) with a defect at second, third, fourth, fifth, and tenth before the termination. Overlaid on this is the real part of the matching impedance from (4). The net reflectance now exhibits a very low values at the resonant frequency for even p, but there are also a series of extra minima distributed across the MIW passband for all p.

Very strong correspondence between the matching impedance and these minima in the reflectance is clear with each minimum when the load resistance is equal to the real part of the matching impedance. At first, this seems somewhat surprising, but since Z_0 has an imaginary component for $\omega \neq \omega_0$, then, to remove all reflectance this must also be matched by its complex conjugate. The load in the defect is pure real but, at these frequencies, the stub between defect and termination can exhibit a pure imaginary impedance which provides this match. The number of frequencies for which matching is thus perfect is now equal to the length of the stub in cells (including the defect). For an odd

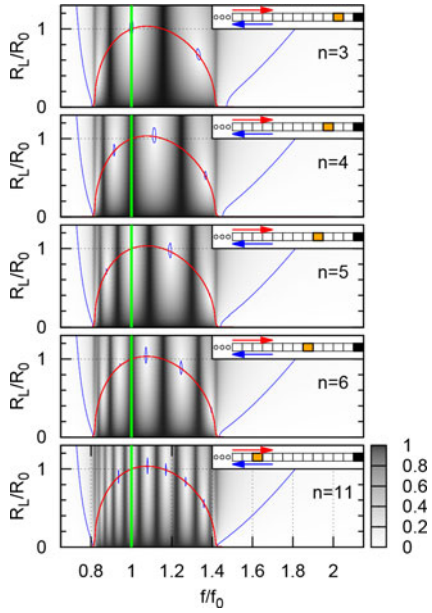

Fig. 3. Net reflectance for the defect and terminated line combined evaluated just before the defect for a low loss MIW ($R \ll \omega_0 M$). Contours at reflectance $=0.04$. Solid curve is the real part of the matching impedance R_0, which shows that zero reflectance nodes correspond to defects having a load equal to R_0. Perfect matching is recovered for cases, where the effective impedance of the remaining line after the defect is zero. For odd numbered cells the match is always possible at f_0.

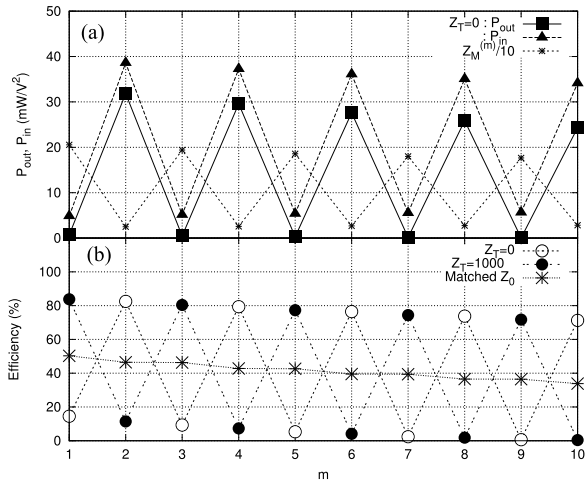

Fig. 4. (a) Input and output power for a 10 cell MIW, at resonant frequency along with input impedance A defect drawing power located at each cell in turn along the line. Cell 10 is the termination and cell 1 is the start of the line where power is injected. The load is equal to R0. Standing waves between the defect and the end of the line have a dramatic impact on the power transfer and impedance. (b) Efficiency calculated for three cases, first when the termination is a short circuit in cell 10 [the case used for (a)], second for the termination being a $1\text{k}\Omega$ pure resistance and third when the final cell is terminated with a matched load.

number of cells, there is no match at resonance, but it is still possible to match at other frequencies. If one instead adds a terminating load to the last cell in the line then power will be absorbed here reducing the overall efficiency for power transfer to the defect, but there will still be solutions to ρ_D that offer zero reflectance off resonance.

C. Net Input Impedance and Power Transfer

Having already determined a method to refer the terminating impedance to any other point on a line it is now possible to complete the calculation for the remaining "m" cell line terminated by Z_M. One may now essentially repeat the process of referring the new termination back to the first cell to which the source is connected as shown in the third line of Fig. 2. Here, we now use (13) with Z_M to find reflectance, then propagate this back to the first cell in the line using (9) (where m replaces p) and finally apply (14) to find the net input impedance of the line at the first cell. Doing this, we derive a final referred impedance for the whole line, including the defect cell as $Z_M^{(m)}$, where the impedance is referred through $m-1$ periods back to cell 1 adjacent to the source cell. Referring everything into the source cell one obtains the source current i_S

$$i_S = \frac{V_S}{R_S + Z + Z_M^{(m)}} \tag{15}$$

where V_S is the source voltage amplitude, while its now possible to determine the input power to the line as $P_{\text{in}} = V_S \Re(i_S)$, we require the output power in order to perform any kind of useful optimization. To this end, having determined the source output one may now find the forward traveling MIW amplitude it induces in the line. To this end, its useful to note that

$$i_S Z_M^{(m)} = X i_1 \tag{16}$$

where we number the cells starting at 0 for the cell to which the source is connected wherein i_S circulates. Writing the MIW amplitudes as incident and reflected waves as before in cell $m-1$, then by considering that cell's kirchoff equation one may obtain an expression for the current in the defect as

$$i_{m-1} = I(1+\rho_D) \tag{17}$$

$$i_{m-2} = I(e^{\gamma d} + \rho_D e^{-\gamma d}) \tag{18}$$

$$i_m = \frac{-Z i_{m-1} - X i_{m-2}}{X} = -\frac{Z}{X} I(1+\rho_D) - I(e^{\gamma d} + \rho_D e^{-\gamma d}) \tag{19}$$

from which output power can be obtained as $P_{\text{out}} = \Re(Z_D)|i_m|^2$. Following this method, Fig. 4(a) shows the input and output powers calculated for a $1V_{\text{rms}}$ source of negligible source impedance with a frequency equal to the resonant frequency of the MIW cells. The source is driving a 10 cell MIW line, terminated with a $Z_D = 0$, formed from resonators with the following properties. Inductance $L = 1.46\ \mu$H, Capacitance $C = 106$ pF, Resistance $R = 1\ \Omega$, mutual inductance $M = 0.37\ \mu$H. In this figure, m is varied to move the defect along the line with $Z_M^{(m)}$, P_{in}, and P_{out} calculated for each configuration. The most obvious feature of this result is the strongly periodic nature of all these parameters resulting from standing waves reflected from the last cell (number 10) in the line, when the receiver is an even number of periods away from the end input and output power is high corresponding to a low value

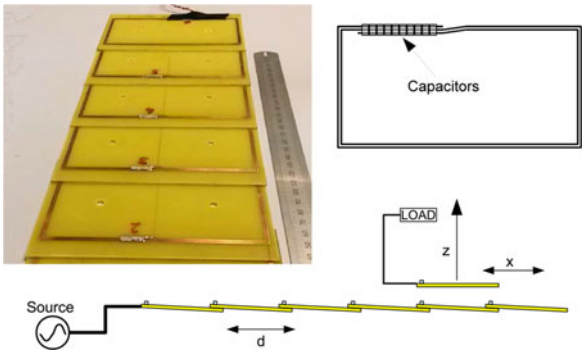

Fig. 5. Magnetoinductive wave power transfer line. Each cell is 150 mm × 74 mm formed from a two turn spiral track of weight 1.2 mm with 0.5 mm between turns. The inner and outer ends of the spiral are bridged by ten ceramic capacitors for tuning and to minimize series losses. Each cell overlaps its neighbors by 2.9 mm.

of the lines input impedance $Z_M^{(m)}$. Output power is extremely low for the odd-numbered cells, which makes the MIW-based wireless power system less attractive in terms of spatial freedom as high performance could only be possible for half the receiver locations. Standing waves are in fact both the cause and the key to solving this problem.

To explore this further, Fig. 4(b) shows the efficiency calculated for three termination cases. First, the same conditions as used for 4(a), where the efficiency is only large for even numbered cells (short circuit (SC) $Z_T = 0$). The second case terminates the line at cell 10 with a high series impedance $Z_T = 1$ kΩ, and the third case is for a perfect termination that matches the MIW impedance wherein there is no reflected wave from the termination as all power is absorbed there. The perfect termination case offers quite uniform power transfer but at relatively low efficiency (<50%), while the two extreme cases of SC and high-impedance termination have large amplitude periodic behavior with peaks >70%. Because of the change in the reflectance produced by the two different termination impedances, the high-efficiency peaks for the high-impedance termination occur where the minima for the SC termination are.

One may understand this effect by considering the magnitude of the current that circulates in the last cell. By adding a large impedance to the last cell the current circulating there is suppressed effectively removing it from the line. Hence, the open-circuit (OC) termination has effectively moved one cell closer to the load changing the phase of the reflected waves arriving there from it. If it was in a location where the reflections destructively interfered with the incident wave amplitude, it now constructively reinforces that amplitude giving higher power transfer.

This result suggests that such a line for 1-D power transfer could indeed offer a uniform high performance as long as the line were to adjust its termination according to the receiver position. Output performance is good when the input impedance of the MIW line is low.

Several important conclusions can be drawn from the reflectance results above:

(1) first, the defect load should match the line impedance to get best performance and reflect no power back to the source;
(2) perfectly terminating a line ($Z_T = Z_0$) to minimize standing waves between the defect (receiver) and the termination removes standing wave effects, but reduces the peak efficiency considerably due to the absorption of power by the termination;
(3) switching the termination impedance from SC ($Z_T = 0$) to OC ($Z_T \gg Z_0$) as a function of the receiver position offers much higher efficiency and power than perfect termination and could be implemented using the input impedance of the line as a detector;
(4) receivers that were able to select two adjacent cells to draw power from could themselves optimize the conditions without need for source measurements;
(5) standing waves that are present when a line is not perfectly terminated will, however, lead to greater power loss in the line's own resistance and may have damage the source if the load is not absorbing the majority of the injected power.

D. Coupled Receiver Model

In the contactless power transfer system under consideration, the power is not merely transferred to a defect resistance in one cell, but is coupled from that cell into a load via a receiver cell. If the receiver has an impedance $Z_R + R_L$, where R_L is the load and $Z_R = R_R + j\omega L_R + 1/j\omega C_R$, and is coupled to the mth cell with a mutual inductance M_X, then the impedance it effectively introduces into that cell is given by

$$Z_D = \frac{\omega^2 M_X^2}{Z_R + R_L}. \tag{20}$$

Having shown that for a low loss line, the optimal defect resistance for power transfer is close to the matching impedance Z_0, we can then determine the constraints on receiver design from (20) by equating Z_D to Z_0, which is equal to $\omega_0 M e^{-\alpha d}$ at resonance. If the receiver is tuned so that its resonance is at the same frequency as the cells in the MIW, then $Z_R = R_R$. Rearranging for the load one finds

$$R_L = \frac{\omega_0 M_x^2}{M e^{-\alpha d}} - R_R. \tag{21}$$

Since the load can never be negative this gives an absolute minimum value for the receiver coupling of $M_X > M R_R/\omega_0$ and effectively defines the maximum height for which the receiver can achieve a perfect match. The maximum value of R_L that can obtain a perfect match is generally dependent on the value of M_X. For a receiver identical to the MIW cells, M_X cannot exceed $\sqrt{L L_R}$ and $R_L^{(\max)} \approx \omega_0 L_R L/M$ assuming that the receiver resistance is negligible in comparison to $\omega_0 M$. Equation (21) suggests that very strong coupling of receiver to line is not essential for good performance, but that the optimal load impedance is strongly dependent on the receiver height. Equation (21) can be used to determine the coupling required for optimum power transfer at the resonant frequency as a function

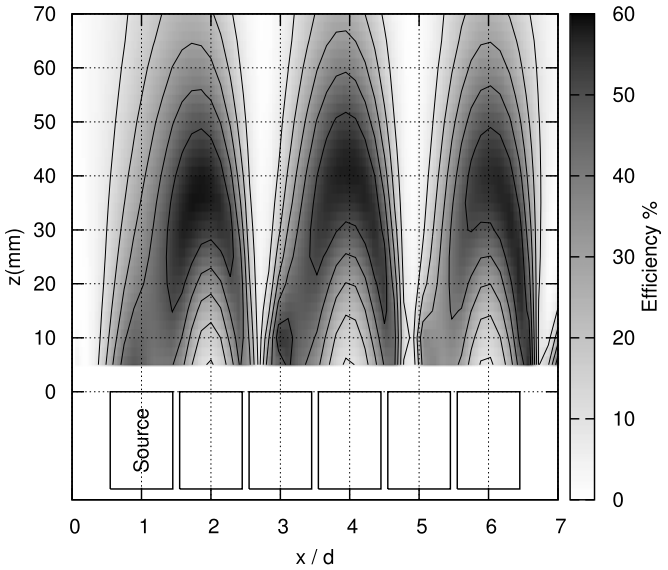

Fig. 6. Measured power transfer efficiencies for a scanned receiver loaded with 10 Ω. Source is connected to the first cell at $x/d = 1$, where d is the cell period on the line (71.1 mm). The termination is at cell 6. Data are shown for the SC termination condition. Peak efficiency occurs at $z = 35$ mm and standing waves cause the peaks in efficiency to be even numbers of cells away from the termination.

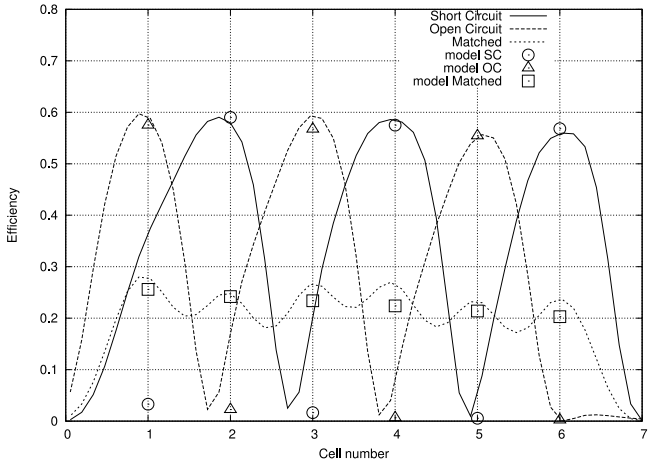

Fig. 7. *Lines:* Measured power transfer efficiencies for the experimental line in SC, OC, and matched termination cases with a 10-Ω load scanned above the line at its optimal height (35 mm). *Points:* Predicted performance using the analytical model for each case. Circles are the model SC termination values, triangles the OC termination predictions, and squares the matched termination case.

of load as

$$M_X^2 = (R_L + R_R)\frac{Me^{-\alpha d}}{\omega_0} \tag{22}$$

in which case it is quite clear that a large load resistance will require much stronger receiver coupling than a smaller one if both are to be driven at maximum efficiency with the same power.

III. Experimental Realization and Results

To test the results of the MIW analysis, we have built a simple 1-D MIW line using printed circuit techniques to fabricate cells for a line (shown in Fig 5). Each cell is 150 × 74 mm and consists of a two turn rectangular spiral track, 1.2 mm wide with a track spacing of 0.5 mm. The cells are tuned to a resonant frequency of 12.8 MHz by soldering ten surface mount ceramic capacitors each of 10 pF across the tracks. Ten parallel capacitors are used to reduce the impact of their equivalent series resistance and contact impedance to maximize the cell's Q factor and keep attenuation to a minimum. Each of these cells has inductance $L = 1.459$ μH, self-capacitance of 6 pF, and a measured effective resistance (derived from a single cell 's Q factor of 120) of $R = 1\ \Omega$.

For our power transfer measurements, we set up a line in which six of these cells are placed such that the two tracks along their neighboring 150 mm long edges overlap (as shown in Fig. 5) giving a mutual inductance of −280 nH and a coupling coefficient $k = -0.38$. In this configuration, second-order coupling is $-2M_2/L = -0.018$ or less than 5% as large as first order, making it a fair match for the first-order model, while it is possible to obtain lines with stronger first-order coupling than this, they often come with the penalty of much greater second-order coupling or a reduction in the maximum possible receiver coupling [22].

Measurements are made using a receiver cell, identical to the line's cells, with either a 10Ω load in series with its LC resonator. The receiver is placed above the line (oriented parallel to the line's cells) and its position is varied along the full length of the line ("*x*" direction) and vertically above it ("*z*" direction). A vector network analyzer (VNA) is used as a source driving the first cell of the line and to measure the received power at the receiver. At each location, in order to obtain a measure for the line's power transfer efficiency both the forward S_{21} and backward S_{11} scattering parameters are measured. These are then used to compute the efficiency according to

$$\eta = \frac{|S_{21}|^2}{(1 - |S_{11}|^2)}\left[1 + \frac{50}{R_L}\right]. \tag{23}$$

For this line, the characteristic impedance according to (4) is 24.6Ω, which means that there is a substantial mismatch between the line and the VNA (impedance 50Ω) leading to an 11% reflection of power back to the source for an infinite line of this type, hence, the correction via S_{11}. Fig. 6 shows the magnitude of the efficiency at resonant frequency derived from (23) for SC termination.

Fig. 6 shows strong impact from standing waves as reflection from the SC termination is very high. Peak efficiency is occurring when the receiver is an even number of cells away from the termination and between 35 and 40 mm above the line. Using (22), one can determine the value of receiver coupling M_X for maximum efficiency to a 10Ω load as 204 nH. Using Fasthenry [26] to determine the variation of mutual inductance between the cells in the axial direction (i.e., between a cell and the receiver placed directly above it), one can find that the predicted mutual inductance for this separation is 197 nH in surprisingly good agreement given the model only includes first-order cou-

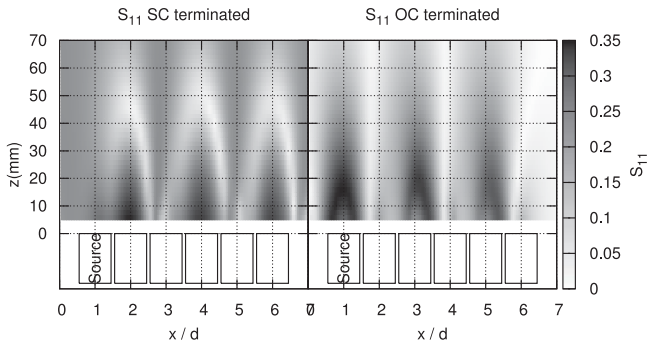

Fig. 8. Scattering parameters measured as the receiver scans the space above the line. Strong reflected signal modulation is present in both termination cases but the peaks of reflected power for SC termination are at even cells and for OC for odd cell numbers.

pling between cells and also between the receiver and the cell directly below it.

Measurements were also made with the same line terminated OC by cutting a gap in the last cell's track just before the capacitors, and in a loaded termination case, where a near matching $22\,\Omega$ resistance was connected across this gap.

Fig. 7Fig. 8shows the efficiency at optimal height versus "x" location for each of the three cases compared to the values derived from the first-order model for an optimal defect load which in this case is equal to 24.6Ω . Agreement between the model calculations (which are valid for receivers located exactly over each of the cell locations in turn), and the peak measured is not perfect but the general trends do match well. Model SC and measured SC terminations show peaks on the same cells with the model SC efficiencies being within 5% of the measured values, although one may expect these to be lower due to secondary coupling effects. The OC case shows its peaks shifted one cell toward the source by the change in termination offering high efficiency for the cells, where SC termination results in a minimum. For both model and experiment, the matched termination results in a relatively low efficiency but a considerable reduction in the modulation.

Based on the efficiency, the current realization is far from optimal but using higher Q resonant coils, and adjusting their dimensions to maximize coupling k, the peak efficiency can be raised considerably as shown in [27].

Results in Fig. 7 show that modulating the termination condition of a line could indeed offer maximum efficiency at all cells. To enable this, one would require a method to detect the receiver position at the source and then a modulated load.

Fig. 8 shows the maps for $|S_{11}|$ for the SC and OC cases. This reflection parameter shows a very strong modulation in the OC and SC cases, but the peaks are different. For most locations on the line switching between the termination conditions would allow a source to select for maximum absorption of power by the load. Methods for measuring reflected power at a source are very straightforward and would then enable a line to adjust its operation to best match a load, maximizing standing wave enhancement of power transfer efficiency.

IV. Conclusion

This paper has introduced a method for modeling MIW-based power transfer lines using closed form analytical expressions without the need for matrix inversion. The model, based on the propagation of MIWs and using only first-order coupling, is a surprisingly good match for experimental results. The model shows that standing waves are a significant problem. To address this issue, adjusting the termination of the final cell in a line was considered, while perfect termination removes all standing waves, it results in rather poor overall efficiency as power is absorbed in the terminating load. If the line is equipped with an adjustable termination capable of switching between low and high impedance, the losses in the termination are always small. Making this switch also switches the standing wave pattern in the line so that if a terminal is in a node for a low-impedance termination it can be powered efficiently by switching to high-impedance termination.

The process whereby the receiver position is detected can be as simple as measuring the reflected power at the source and establishing the line's input impedance. Another solution would be to change the power supply frequency to maintain optimum power transfer and in this case a source would have to first establish the input impedance for the resonant frequency. Based on the results of Fig. 4, a low value would correspond to a case, where the receiver is located in a standing wave node and the alternate frequency selected.

Other work has considered [7] using two receivers adjacent to one another, and combining the power they receive so as to smooth out the effects of standing waves. To model this, one may use the same model as already described, but now the two receiver's respective loads appear in adjacent cells. When one is in a standing wave node the other will of course be in an antinode resulting in a simple guarantee of optimal power transfer. Such a facile solution results in a larger overall receiver footprint and may suffer from secondary coupling between the receivers themselves.

One perspective on relay coil/MIW lines is that they are a series of distributed transformers and the issue of transformer action is then worth considering. If a load is presented to the line while it is powered, MIW reflected from that load return toward the source, modifying the input impedance and increasing the power drawn from the source. The phase of the reflected waves arriving at the source will determine the impact of applying the load. Changes in the demand for a load are communicated by the reflected MIW propagating back to the source, but this is not an instantaneous process. MIW are slow waves and for narrowband (weakly coupled $k \ll 1$) systems their velocity can be very low. This could be of concern, where loads are being driven whose demand varies very rapidly in large MIW systems although most current demonstrations are probably too small for this to become a serious issue.

Finally, by using the physics of MIW to determine input impedance without the need to use either impedance matrix inversion or to sum a finite continuous fraction, a general solution to the finite continuous fraction has been obtained. This method to determine input impedance allows analysis of far more than

the situation described in this paper, sources at any point on a line, multiple sources and receivers may all be studied using this technique while still maintaining a relatively simple set of analytical formulas.

REFERENCES

[1] N. Tesla, "The transmission of electric energy without wires," *Electr. World Eng.*, vol. 5, pp. 162–167, 1904.

[2] A. Kurs, A. Karalis, R. Moffatt, J. D. Joannopoulos, P. Fisher, and M. Soljavci, "Wireless power transfer via strongly coupled magnetic resonances," *Science*, vol. 317, no. 5834, pp. 83–86, 2007.

[3] D. van Wageningen and T. Staring, "The Qi wireless power standard," in *Proc. 14th Int. Power Electron. Motion Control Conf.*, 2010, pp. S15–25.

[4] R. Tseng, B. von Novak, S. Shevde, and K. A. Grajski, "Introduction to the alliance for wireless power loosely-coupled wireless power transfer system specification version 1.0.," in *Proc. IEEE Wireless Power Transfer*, 2013, pp. 79–83.

[5] Y. Urzhumov and D. R. Smith, "Metamaterial-enhanced coupling between magnetic dipoles for efficient wireless power transfer," *Phys. Rev. B*, vol. 83, no. 20, pp. 205114-1–205114-10, 2011.

[6] C. J. Stevens, "Power transfer via metamaterials," *Comput. Mater. Contin.*, vol. 33, no. 1, pp. 1–18, 2013.

[7] B. Wang, W. Yerazunis, and K. H. Teo, "Wireless power transfer: Metamaterials and array of coupled resonators," *Proc. IEEE*, vol. 101, no. 6, pp. 1359–1368, Jun. 2013.

[8] S. Y. R. Hui, W. Zhong, and C. K. Lee, "A critical review of recent progress in mid-range wireless power transfer," *IEEE Trans. Power Electron.*, vol. 29, no. 9, pp. 4500–4511, Sep. 2014.

[9] Y. Lim, H. Tang, S. Lim, and J. Park, "An adaptive impedance-matching network based on a novel capacitor matrix for wireless power transfer," *IEEE Trans. Power Electron.*, vol. 29, no. 8, pp. 4403–4413, Aug. 2014.

[10] C. K. Lee, W. X. Zhong, and S. Y. R. Hui, "Effects of magnetic coupling of nonadjacent resonators on wireless power domino-resonator systems," *IEEE Trans. Power Electron.*, vol. 27, no. 4, pp. 1905–1916, Apr. 2012.

[11] Y. Narusue, Y. Kawahara, and T. Asami, "Impedance matching method for any-hop straight wireless power transmission using magnetic resonance," in *Proc. IEEE Radio Wireless Symp.*, 2013, pp. 193–195.

[12] K. Mori, H. Lim, S. Iguchi, K. Ishida, M. Takamiya, and T. Sakurai, "Positioning-free resonant wireless power transmission sheet with staggered repeater coil array (SRCA)," *IEEE Antennas Wirel. Propag. Lett.*, vol. 11, pp. 1710–1713, 2012.

[13] S. Raju, R. Wu, M. Chan, and C. P. Yue, "Modeling of mutual coupling between planar inductors in wireless power applications," *IEEE Trans. Power Electron.*, vol. 29, no. 1, pp. 481–490, Jan. 2014.

[14] E. Shamonina, V. A. Kalinin, K. H. Ringhofer, and L. Solymar, "Magnetoinductive waves in one, two, and three dimensions," *J. Appl. Phys.*, vol. 92, no. 10, pp. 6252–6261, 2002.

[15] C. J. Stevens, C. W. Chan, K. Stamatis, and D. J. Edwards, "Magnetic metamaterials as 1-D data transfer channels: an application for magneto-inductive waves," *IEEE Trans. Microw. Theory Tech.*, vol. 58, no. 5, pp. 1248–1256, May 2010.

[16] E. Shamonina, V. Kalinin, K. H. Ringhofer, and L. Solymar, "Magneto-inductive waveguide," *Electron. Lett.*, vol. 38, no. 8, pp. 371–373, 2002.

[17] C. W. T. Chan, and C. J. Stevens, "Two-dimensional magneto-inductive wave data structures," in *Proc. 5th Eur. Conf. Antennas Propag.*, 2011, pp. 1071–1075.

[18] M. Wiltshire, J. Hajnal, J. Pendry, D. Edwards, and C. Stevens, "Metamaterial endoscope for magnetic field transfer: Near field imaging with magnetic wires," *Opt. Exp.*, vol. 11, no. 7, pp. 709–715, Apr. 2003.

[19] C. J. Stevens, C. W. Chan, K. Stamatis, and D. J. Edwards, "Magnetic metamaterials as 1-D data transfer channels: An application for magneto-inductive waves," *IEEE Trans. Microw. Theory Tech.*, vol. 58, no. 5, pp. 1248–1256, May 2010.

[20] O. Sydoruk, O. Zhuromskyy, E. Shamonina, and L. Solymar, "Phonon-like dispersion curves of magnetoinductive waves," *Appl. Phys. Lett.*, vol. 87, no. 7, pp. 072501–072501, 2005.

[21] A. Radkovskaya, M. Shamonin, C. J. Stevens, G. Faulkner, D. J. Edwards, E. Shamonina, and L. Solymar, "An experimental study of the properties of magnetoinductive waves in the presence of retardation," *J. Magn. Magn. Mater.*, vol. 300, no. 1, pp. 29–32, 2006.

[22] R. R. A. Syms, L. Solymar, I. R. Young, and T. Floume, "Thin-film magneto-inductive cables," *J. Phys. Appl. Phys.*, vol. 43, no. 5, p. 055102, 2010.

[23] X. Zhang, S. L. Ho, and W. N. Fu, "Quantitative design and analysis of relay resonators in wireless power transfer system," *IEEE Trans. Magn.*, vol. 48, no. 11, pp. 4026–4029, Nov. 2012.

[24] R. R. A. Syms, I. R. Young, and L. Solymar, "Low-loss magneto-inductive waveguides," *J. Phys. Appl. Phys.*, vol. 39, no. 18, pp. 3945–3951, 2006.

[25] L. Solymar, *Waves in Metamaterials*. London, U.K.: Oxford Univ. Press, 2009.

[26] M. Kamon, M. J. Tsuk, and J. K. White, "FASTHENRY: A multipole-accelerated 3-D inductance extraction program," *IEEE Trans. Microw. Theory Tech.*, vol. 42, no. 9, pp. 1750–1758, Sep. 1994.

[27] W. Zhong, C. Lee, and R. Hui, "General analysis on the use of tesla' s resonators in domino forms for wireless power transfer," vol. 60, no. 1, pp. 261–270, Jan. 2013.

Christopher J. Stevens received the Graduate degree (first class Hons.) in physics from the University of Oxford, Oxford, U.K., in 1990, and the D.Phil. degree in condensed matter physics, in 1994, following a three-year doctoral degree course at the same university.

He worked with Uiversita Degli Studidi Lecce on the properties of wide band gap semiconductor materials. He was a post doctoral fellow in the Clarendon laboratory on the dynamic properties of high temperature superconductors, after which he held a Royal Academy of Engineering fellowship at St Hugh's college, Oxford. During this period, he developed a number of novel devices based on kinetic inductance and photomixing effects. His current research activities include ultrawideband communications, metamaterials, ultrafast nanoelectronics, and high-speed electromagnetics. He is an Associate Professor of Engineering Science at the University of Oxford, Oxford, U.K., and is a Fellow of St. Hughs College, Oxford. He received awards for practical physics.